CORE
Metadata, citation and similar papers at core.ac.uk
Provided by Electronic Sumy State University Institutional Repository

PROCEEDINGS OF THE INTERNATIONAL CONFERENCE NANOMATERIALS: APPLICATIONS AND PROPERTIES
Vol. 1 No 3, 03TF23(4pp) (2012)

Substructural Features of $Zn_{1-x}Mn_xTe$ Solid Solution Thin Films

D.I. Kurbatov[1], O.V. Klymov[1], A.S. Opanasyuk[1], S.M. Danilchenko[2], H.M. Khlyap[3]

[1] *Sumy State University, 2, Rymsky Korsakov Str., 40007 Sumy, Ukraine*
[2] *Institute of Applied Physics the NAS of Ukraine, 58, Petropavlovska Str., 40030 Sumy, Ukraine*
[3] *TU Kaiserslautern, Distelstr.11, D-67657, Kaiserslautern, Germany*

(Received 11 August 2012; published online 26 August 2012)

The substructural characteristics of $Zn_{1-x}Mn_xTe$ films deposited by closed space vacuum sublimation method under various condensation conditions are investigated. Sizes of the coherent scattering domain size, microdeformation degree, staking fault defects' concentration in the condensates, the averaged dislocation density at the subgrain boundaries and in their bulk as well as the total dislocation concentration are determined by the physical broadening of the X-ray lines using the Cauchy and gauss approximations and the threefold function convolution method. The calculations are compared with data for undoped ZnTe. It is found out that the Mn-doping causes some degradation of structural characteristics of the condensates compared with undoped layers.

Keywords: Substructure, X-ray diffraction patterns, Microdeformations, Orientation factor.

PACS numbers: 61.05.cp, 61.72.uj

1. INTRODUCTION

Semimagnetic semiconductor solid solutions are attract the researchers' attention due to their unique photoluminescent, magnetic and magneto-optical properties of the material suitable for designing devices for micro(opto)electronics, photovoltaics and spintronics [1, 2]. The effectivity of these devices depends on the transport properties of the free charge carriers (by the product of the mobility and the lifetime $\mu\tau$), which in turn are determined by recombination centers' concentration in the material [3, 4]. As the recombination centers affecting the carrier lifetime in the semiconductor are the surface, grain boundaries, dislocations, SF defects, point defects of various nature (both native and impurity-caused ones) and other imperfectness of the crystalline structure, the optimized structural features of the films are necessary [4].

However, producing $Zn_{1-x}Mn_xTe$ films with controllable Mn content and optimized characteristics is a challenge while the components' pressures are considerably different. Thus, these layers are mostly deposited by laser [5] and flash evaporation [6], high frequency magnetron scattering [7], MOVPE [8], which are characterized by the high non-equilibrium of the process. Low quality of the layers with a fine structure does not allow using them for photodetectors, hard radiatopn detectors and solar cells.

Authors [5-8] have investigated some structural features of $Zn_{1-x}Mn_xTe$ films. However, their substructural characteristics (coherent scattering domain (CSD) size, microdeformation grade (or degree) caused by the dislocation presence) are not studied until recently. There is a motivation of this work: investigation of influence of the physical technological conditions of condensation on substructural characteristics of the layers obtained by the closed space vacuum sublimation (CSVS). This technique allows obtaining multi-component films under quasi-equilibrium conditions for growth of structurally perfect layers [9-10]. Experimental results are compared with those obtained for undoped ZnTe films.

2. EXPERIMENTAL DETAILS

Thin $Zn_{1-x}Mn_xTe$ films were deposited on cleaned glass substrates under residual gas pressure no more than $5\cdot10^{-3}$ Pa. The detailed description of the growth setup is done elsewhere [11-12]. The charge of semiconductor purity with 10% Mn content was evaporated under the evaporator temperature T_e = 1073 K. The substrate temperature was changed in the interval T_s = (423-823) K, t = 15 min.

The structural investigations of the films were performed by using the diffrctometer DRON 4-07 in Ni-filtered K_α radiation of the copper anode in the angle range 2θ from 10^0 to 80^0, where 2θ is the Bragg angle. The focusing procedure was according to the Bragg-Brentano mode. The experimental curves were normalized by the intensity of the (111) peak of the cubic phase. The phase analysis was done by comparison of interplane distances and arbitrary intensities of the X-ray peaks from the examined samples and the etalon according to the JCPDS data [13]. The XRD method was also applied for determining the arbitrary size L of CSD and the microdeformation grade ε in thin films $Zn_{1-x}Mn_xTe$ by the broadening of the XRD lines. To resolve the diffraction broadening caused by the physical (β) instrumental (b) effects we have used Cauchy and Gauss approximations [14-15]. Besides that, the parameters mentioned above were found by the threefold convolution method [16]. To take into account the contribution of the instrumental effect in the X-ray line broadening we have measured the width b of the corresponding reflexes of the etalon (the etched ZnTe charge). All procedures of the working-out the X-ray line profiling (background removing, smoothing, K_α doublet resolution) were performed using the software DIFWIN-1.

It is known that the CSD boundaries are formed by the dislocations located at their boards, at the same time, the dislocations in the subgrain bulk lead to microdeformations in the material. It makes possible to estimate the arbitrary dislocation density using the values L and ε according to the microdeformation value ε and the CSD size L in the films. The averaged through

 © 2012 Sumy State University

the sample density of the dislocations formed the subgrain boundaries is [17-18]

$$\rho_L = \frac{3n}{L^2}, \qquad (1)$$

where n is a number of dislocations on the each face of the six planes of the block.

If the dislocations are mostly located in the middle of the subgrains the dislocation density is obtained from the expression [17-18]

$$\rho_\varepsilon = \frac{K}{F}\left(\frac{2\varepsilon}{b}\right)^2, \qquad (2)$$

where 2ε is a width of the microdeformation distribution; F is a constant taking into account the increase of the dislocation energy under interaction with other dislocations; b is a modulus of the Burgers vector; K is a constant depending on the dislocation distribution function. K=25 for the Cauchy function and K=4 for the Gauss curve.

Accepting $n = F = 1$ expressions (1), (2) give an estimation the lower limit of ρ_L and the upper limit of ρ_ε.

Somewhat other expression for estimation the total dislocation concentration in the material is given in [19]:

$$\rho = \frac{15\varepsilon}{d_0 L}. \qquad (3)$$

Thus, expressions (1) – (3) make it possible to estimate the concentration of dislocations in the CSD bulk, at their boundaries, and the total concentration.

Supposing the CSD s are of equal axes and the additional broadening of (111) and (222) X-ray lines compared with (200) and (400) lines is due to the SF presence one can calculate the total concentration of the deformation and growth defects in $Zn_{1-x}Mn_xTe$ films [17-18]

$$\alpha' = 1{,}5\alpha + \beta = 3{,}04\left(\frac{1}{L_{h00}} - \frac{1}{L_{hhh}}\right) d_{111}, \qquad (4)$$

where α is the growth defects' concentration, β stands for the SF concentration, and $d_{(111)}$ is an interplane distance.

3. INTERPRETATION OF EXPERIMENTAL RESULTS

As we have shown earlier [20], the grown $Zn_{1-x}Mn_xTe$ films had the polycrystalline structure of stable cubic modification with 1.61-3.04 at. % Mn in composition. Fig. 1 plots the X-ray diffraction patterns from ZnTe<Mn> films deposited under various substrate temperatures. Under thickness $d \sim$ 2-4 μm they had the grain size D = 0.50-1.12 μm which has increased at the substrate temperature elevation and closing condensation conditions to the equilibrium ones.

As is known, the X-ray line broadening is caused not only by the instrumental effects but also by small CSD sizes (L), the microdeformations ($\varepsilon = \Delta d/d$) and the distortions of the crystal lattice, in our case the SF. The arbitrary CSD size L and the microdeformation grade ε in $Zn_{x-1}Mn_xTe$ condensates was made by the physical

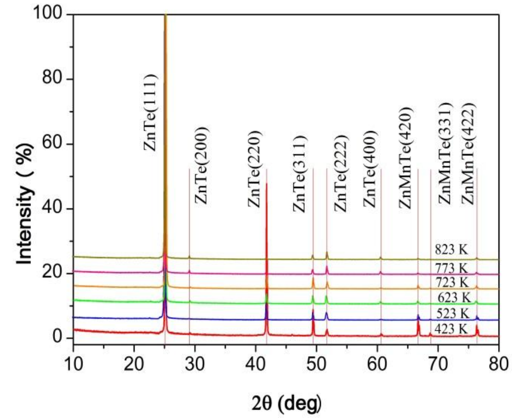

Fig. 1 – X-ray diffraction patterns from $Zn_{x-1}Mn_xTe$ films deposited under various physical technological regimes

broadening of (111)-(222) (200)-(400) X-ray diffraction peaks of the cubic phase. This procedure has allowed defining the substructural parameters of the films in directions normal to these crystallographic planes. Table 1 lists the results obtained by the Cauchy and Gauss approximations as well as the more precise data from the X-ray line threefold convolution method. Fig.2 shows results of comparison made for the CSD size and microdeformation grade in ZnTe and $Zn_{1-x}Mn_xTe$ films calculated using three approximations: Cauchy, Gauss and threefold convolution.

Table 1 and Fig.2 point out the CSD sizes and microdeformation values calculated by the threefold convolution method are intermediate between the data produced by the Cauchy and Gauss approximations having a good correlation. Further we discuss the results from the threefold convolution method as the most precise ones [16].

As is seen from the Table 1 and Fig.2, under elevating T_s the CSD size increases from $L \sim 97$ nm up to ~110 nm, then it decreases down to ~ 75 nm in direction normal to the (111) planes in $Zn_{1-x}Mn_xTe$ films (Fig.2a). The maximal size exists under optimal temperature region (T_s = 600-650 K). At the same time, the microdeformation grade in this direction decreases under increasing T_s from $\varepsilon \sim 2.0\cdot10^{-3}$ to $\varepsilon \sim 1.2\cdot10^{-3}$ (Fig.2b).

These results are in a good agreement with those obtained earlier for undoped ZnTe films [21-22], where the functions L-T_s and ε-T_s were similar (Fig. 2 a,b, curve 4). We should note that the optimal deposition temperatures are the same for preparing the films with maximum CSD sizes for both undoped and Mn-doped ZnTe layers. At the same time, $Zn_{1-x}Mn_xTe$ films had the larger CSD size and microdeformation grade compared with ZnTe films (Fig.2, a, b).

Using the known microdeformation values and the expression $\sigma = E\varepsilon$ we have calculated the microstress grade in the condensates $Zn_{1-x}Mn_xTe$ (Table 1). We have used the Yung modulus value (E = 64 GPa) obtained under calculating the mechanical constants for ZnTe [21-22]. It is shown that the microstress grade in $Zn_{1-x}Mn_xTe$ films changes in the interval σ = 67.5-130.7 MPa. These values are also larger than those in undoped ZnTe films (σ = 20-83 MPa).

Table 1 – Substructural characteristics of $Zn_{1-x}Mn_xTe$ thin films

T_s, K	(*hkl*)	*L*, nm			$\varepsilon\cdot 10^3$			α'%
		Approximation by		From convolution	Approximation by		From convolution	
		Gauss	Cauchy		Gauss	Cauchy		
423	(111)-(222)	82.5	147.0	96.6	2.3	1.7	2.0	0.05
	(200)-(400)	97.9	126.0	101.0	0.9	0.4	0.7	
523	(111)-(222)	82.6	154.4	99.3	2.5	1.9	2.2	1.37
	(200)-(400)	43.4	38.4	43.7	1.2	0.9	2.2	
623	(111)-(222)	92.0	169.3	109.7	2.2	1.6	1.9	0.78
	(200)-(400)	57.6	81.5	61.1	1.9	1.2	1.6	
723	(111)-(222)	63.8	86.9	66.8	1.9	1.1	1.5	0.57
	(200)-(400)	86.1	161.3	103.6	2.1	1.5	1.8	
773	(111)-(222)	70.0	87.7	71.8	1.4	0.6	1.1	0.07
	(200)-(400)	71.6	98.8	75.4	1.5	0.8	1.2	
823	(111)-(222)	71.8	94.3	74.5	1.5	0.8	1.2	0.27
	(200)-(400)	59.3	82.5	62.5	1.8	1.1	1.5	

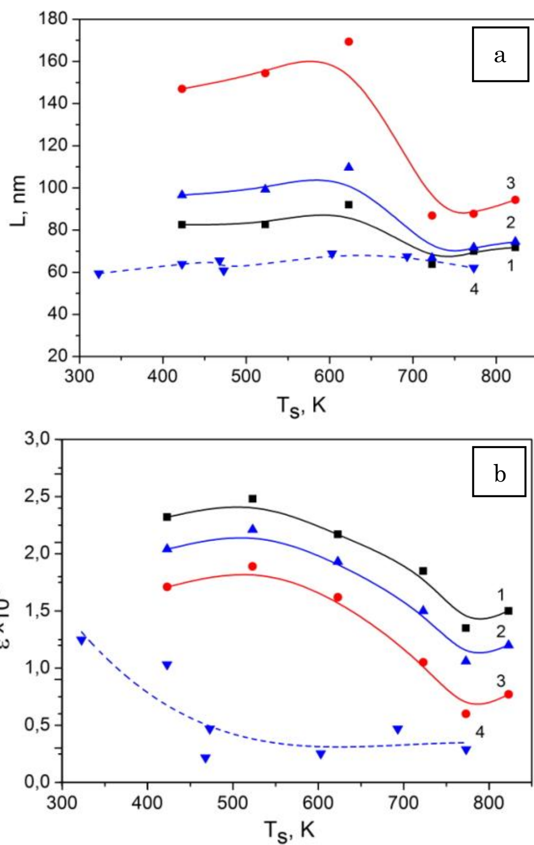

Fig. 2 – The effect of the substrate temperature T_s on the CSD size (a) and the microdeformation grade (b) of the films $Zn_{1-x}Mn_xTe$ (1-3) and ZnTe (4). The approximation is done according to Cauchy (1), Gauss (3), and to the method of three-fold convolution (2)

Three different ways of the CSD size calculation show a typical feature: the calculated values $L_{(h00)} > L_{(hhh)}$. Suppose as in [11-12, 21-22] that the CSD have equal axes but the SF mainly contribute to the line broadening responsible for the reflection from the (*hhh*) planes. Then it is possible to determine the total concentration of deformation and growth defects α' in $Zn_{1-x}Mn_xTe$ films according to the expression (4). These results are listed in Table 1.

As is seen, the arbitrary SF concentration in $Zn_{1-x}Mn_xTe$ films decreases as the substrate temperature increases from 1.37% (T_s = 523 K) up to 0.27% (T_s = 823 K). These values are somewhat larger than those calculated for the undoped ZnTe films: 0.67% (T_s = 323 K) – 0.04 (T_s = 693 K) [21-22].

Table 2 and Fig.3 illustrate results of calculating concentration of dislocations at the CSD boundaries, in the CSD bulk and the total dislocation concentration in $Zn_{1-x}Mn_xTe$ films made according to the expressions (1)-(3). As is seen, the data have a good correlation within order of magnitude. These films are characterized by considerably low value of the dislocation concentration $\rho_{L\varepsilon}$= (6.8-9.6)$\cdot 10^{14}$ (see, for example, [23], where for ZnTe films ρ = (6.3-16.6)$\cdot 10^{14}$ lin/m^2). As the substrate temperature elevates, the total dislocation concentration in the solid solution films defined from the (111-(222) reflexes is decreasing (Fig.3). However, this value is appeared as the larger one than that in ZnTe films $\rho_{L\varepsilon}$ = (7.8-21.4)10^{-13} lin/m^2. Thus, the manganese doping leads to the degradation of the substructure of ZnTe films: the microdeformations and microstresses as well as the concentration of the SF and dislocations are increased.

Table 2 – Microdeformations and dislocation density in $Zn_{1-x}Mn_xTe$ films

T_s, K	(*hkl*)	*L*, nm	ε 10^3	σ, MPa	ρ_L, 10^{14} lin/m^2	ρ_ε, 10^{14} lin/m^2	$\rho_{L\varepsilon}$, 10^{14} lin/m^2
423	(111)-(222)	96.6	2.0	130.7	3.2	4.9	9.0
523	(111)-(222)	99.3	2.2	141.4	3.0	5.7	9.5
623	(111)-(222)	109.7	1.9	123.4	2.5	4.4	7.5
723	(111)-(222)	66.8	1.5	96.1	6.7	2.7	9.6
773	(111)-(222)	71.8	1.1	67.5	5.8	1.3	6.3
823	(111)-(222)	74.5	1.2	76.6	5.4	1.7	6.8

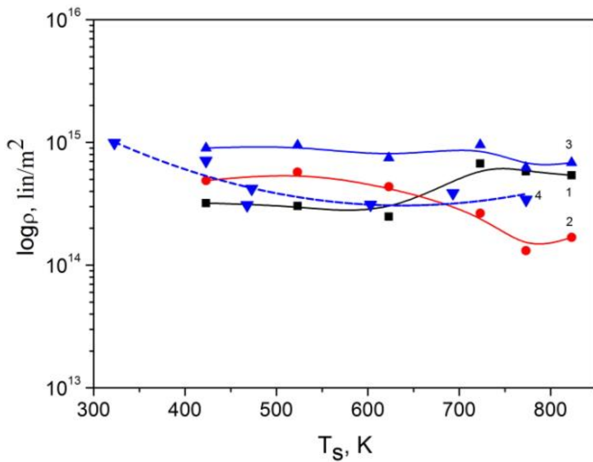

Fig. 3 – Dependence of the dislocation concentration on the substrate temperature in $Zn_{1-x}Mn_xTe$ (1-3) and ZnTe (4) films: at the subgrain boundaries (1), in their bulk (2) and the general dependence (3, 4) using the reflexes (111)-(222).

4 CONCLUSIONS

Thin films $Zn_{1-x}Mn_xTe$ are prepared by thermal evaporation in closed space under various conditions of the condensation. The substructural characteristics of these layers are examined by means of the XRD method. The CSD sizes, the microdeformation grade, the concentration of the SF (stacking faults) in the condensates, the arbitrary dislocation density at the subgrain boundaries and in the bulk of the films are determined by the physical broadening of the diffraction lines using three different approximations for the line profile. It is shown that the dependence of the CSD size on the substrate temperature is a non-linear function with a maximum at T_s =550-600 K. The largest values of L determined by the threefold convolution method reach 109.7 nm. The microdeformation grade in the films decreases as the substrate temperature T_s from $\varepsilon \sim 2.0\cdot 10^{-3}$ up to $\varepsilon \sim 1.2\cdot 10^{-3}$. It is found out that the films $Zn_{1-x}Mn_xTe$ are characterized by low concentration of dislocations ($\rho_{L\varepsilon}$= (6.8-9.6)$\cdot 10^{14}$ lin/m^2) and SF (α'=0.27%-1.37%) compared with the layers deposited by other methods. These results point out the more equilibrium condensation conditions of the films of the solid solution under its evaporation in vacuum closed space and the technological perspectives for preparing condensates with the highest structural perfectness for practical microelectronic applications. At the same time, the manganese doping of ZnTe films leads to the degradation of their substructural characteristics in comparison with the undoped condensates.

AKNOWLEDGEMENTS

Work performed under the state budget project № 68.03.01.10-12 Ministry of Education Youth and Sports of Ukraine and with the support of the State Agency for Science, Innovation and Informatization of Ukraine.

REFERENCES

1. J. Kossut, J.A Gaj., *Introduction to the Physics of Diluted Magnetic Semiconductors, Springer Series in materials science* (Warsaw: 2010).
2. A. Avdonin, *Properties of ZnMnTe alloy doped with oxygen and chromium* (Warsaw: 2010).
3. A. Owens, A. Peacock, *Nucl. Instrum. Meth. B* **531**, 18 (2004).
4. W.K. Metzger, D. Albin, D. Levi, P. Sheldon, X. Li, *J.Appl. Phys.* **94** No 5, 3549 (2003).
5. H.J. Masterson, J.G. Lunney, *Appl. Surf. Scien.* **86**, 154 (1995).
6. G. Romera-Guereca, J. Lichtenberg, A. Hierlemann, D. Poulikakos, B. Kang, *Experimental Thermal and Fluid Science* **30**, 829 (2006).
7. D. Zeng, W. Jie, H. Zhou, Y. Yang, *Nucl. Instrum. Meth. A,* **614**, 68 (2010).
8. A. Zozime, M. Seibt, J. Ertel, A. Tromson-Carli, R. Druilhe, C. Grattepain, R. Triboulet, *J. Crystal Growth* **249**, 15 (2003).
9. A. Lopez-Otero, *Thin Solid Films* **49**, 3 (1978).
10. I.P. Kalinkin, V.B. Aleskovskij, A.V. Symashkevich, *Epitaxial A_2B_6 films* (Leningrad, LGU, 1978) (in Russian).
11. V.V Kosyak, A.S. Opanasyuk, P.M. Bukivskij, Yu.P. Gnatenko. *J. Cryst. Growth* **312**, 1726 (2010).
12. D. Kurbatov, H. Khlyap, A. Opanasyuk. *phys. status solidi a* **206** No7, 1549 (2009).
13. *Selected powder diffraction data for education straining (Search manual and data cards)* (USA: International Centre for diffraction data: 1988).
14. B.E. Warren, *X-ray Diffraction.* (New York: Dover: 1990).
15. D.K. Bowen, K. Brian Tanner. *X-Ray Metrology in Semiconductor Manufacturing.* (Taylor & Francis Group: 2006)
16. S.N. Danilchenko, O.G. Kukharenko, C. Moseke. *Cryst. Res. Technol.* **37** № 11, 1234 (2002).
17. L.S. Palatnik, M.Ya. Fuchs, V.M. Kosevich, *The mechanism of formation and Substructure of Condensed Films* (Moscow: Science: 1972) (in Russian).
18. D. Kurbatov,V. Kosyak, M. Kolesnyk, A. Opanasyuk, S. Danilchenko*, Integreted Ferroelectrics* **103***,* 1 (2008)
19. T. Mahalingam, V.S. John, G. Ravi, P.J Sebastian. *Cryst. Res.Technol.* **37** No4, 329 (2002).
20. D.I. Kurbatov, O.V. Klymov, A.S. Opanasyuk, A.G. Ponomarev, P.M. Fochuk, H.M. Khlyap, *Hard X-Ray, Gamma-Ray, and Neutron Detector Physics XIV, 12-16 August 2012, San Diego Convention Center*, (San Diego, CA United States).
21. M.M. Kolesnyk, S.M. Danilchenko, A.S. Opanasyuk, N.M. Opanasyuk, *Vesnik Sumy State University. Series: Physics, Mathematics, Mechanics*, **2**, 90 (2008) (in Ukrainian).
22. M.M. Kolesnyk, D.I. Kurbatov, A.S. Opanasyuk, V.B. Loboda, *Semiconductor Physics, Quantum Electronics & Optoelectronics* **12** No1, 35 (2009.)
23. T. Mahalingam, V.S. John, G. Ravi, *Cryst. Res. Technol.* **37** No4, 329 (2002).